

Fluctuating forces caused by internal two-phase flow on bends and tees

J.L. Riverin^a, E. de Langre^{a,b,*}, M.J. Pettigrew^a

^a*BWC/AECL/NSERC Chair of Fluid-Structure Interaction, Department of Mechanical Engineering, Ecole polytechnique, Montréal, QC, Canada H3C 3A7*

^b*Department of Mechanics, LadHyX, Ecole polytechnique, 91128 Palaiseau, France*

Received 1 August 2005; received in revised form 20 April 2006; accepted 12 June 2006

Abstract

The time-dependent forces resulting from a two-phase air–water mixture flowing in an elbow and a tee are measured. Their magnitudes as well as their spectral contents are analyzed. Comparison is made with previous experimental results on similar systems. For practical applications a dimensionless form is proposed to relate the characteristics of these forces to the parameters defining the flow and the geometry of the piping. Using a momentum balance we show that these forces are correlated with local measurements of the void fraction in the flow.

© 2006 Elsevier Ltd. All rights reserved.

1. Introduction

Two-phase flow is found in many systems used in nuclear and chemical engineering. Mixtures of liquid and gas may be steam and water, such as in heat-transfer apparatus, or non-miscible products such as in offshore production. Some aspects of the excitation of structures by these two-phase flows are known to be related to the existence of distinct phases with distinct densities. This has been analyzed in the case of flow external to the structure, such as in heat exchangers where steam and water flow through a tube bundle (see Ref. [1] for a review).

In the case of internal flow in piping systems, excitation forces materialize at flow-turning elements such as bends, elbows and tees. Much less attention has been paid to this case. The first set of experiments aimed at characterizing these forces was conducted by Yih and Griffith [2] in relation with nuclear engineering. By measuring forces on tees subjected to ascending air–water mixtures they found that fluctuating forces were of the same order as the load induced by the steady component of the flow. A dimensionless expression was proposed to relate experiments with various diameters and flow velocities. Using a momentum balance these forces were related to the time variation of the density of the fluid entering the tee, liquid and gas alternating. In term of spectral content, a dominant frequency emerged, and was considered as rather low in comparison

*Corresponding author. Department of Mechanics, LadHyX, Ecole polytechnique, 91128 Palaiseau, France. Tel.: +33 1 69 33 36 01; fax: +33 1 69 33 30 30.

E-mail address: delangre@ladhyx.polytechnique.fr (E. de Langre).

with those typical of piping elements. This probably led to the common idea in the field of nuclear engineering that such excitations were of minor practical importance. In recent experiments Riverin and Pettigrew [3] showed that the induced forces can nevertheless be of significant magnitude and that strong vibrations of U-bends can be caused by such two-phase flows.

In the field of chemical engineering concerns about these fluctuating forces arose more recently, from failures of piping systems, see Tay and Thorpe [4] and references therein. In the design of such piping values of the maximum possible load are sought, to prevent fracture. These loads are typically related to the passage of slugs through bend, as discussed in Refs. [4,5]. A recent experimental program has been reported in Ref. [4] where a horizontal bend is subjected to slugs of liquids. Using also a momentum balance, the measured forces were found to be closely related to the dynamics of the slugs, which was simultaneously measured. The effect of surface tension and of viscosity of the liquid phase were tested and found to be of minor importance. In Refs. [6–8], a detailed experimental analysis of the flow motion and fluctuations in a Tee-junction has been presented. Pressure fluctuations in the outlet branches have been analysed in terms of magnitude and of spectral content, but no forces have been directly measured. These results will be reconsidered in Section 5 in relation with our findings.

Considering all these results it appears that a common mechanism of excitation was observed in quite different systems: (a) a tee subjected to vertical flow, at high velocities (more than 15 m/s) with diameters smaller than 25 mm in Yih and Griffith [2], (b) a bend subjected to horizontal flow of slugs with low velocities (less than 4 m/s) with a larger diameter of 70 mm. The aim of the present work is to arrive at a common formulation of these forces, in dimensionless form so that it can be used in practical applications in piping design. In particular we seek to characterize the rms value and the spectral content of these excitations.

A computational approach to this question is possible but would raise several difficulties. First of all, as we seek values of the fluctuation load, time-dependent computational results are needed on a duration such that the spectral analysis can be made accurately. Second, the nature of the flow regimes considered here (bubbly, churn or slug) are such that the complexity in time and space of the interface between gas and liquid would require considerable space and time refinement in the numerical technique [9]. Note here that simpler homogenized flow models where the interface positions are not explicitly computed would not allow to derive the fluctuating loads, as these loads are not caused by turbulence but by alternating of phases. Finally the geometry of bends and tees is such that flow patterns are quite complex even in their time-averaged characteristics. Recent computations, such as in Supa-Amornkul et al. [10] or Adechy and Issa [11] and reference therein, show that the computational derivation of the spectral content of fluctuating forces on bends and tees does not seem presently feasible. We therefore use here an experimental approach.

The existing experimental data on forces acting on bends and tees are few, and are based on experiments either on bends or on tees. To our knowledge no experiment has been done on bends and tees in the same flow regime and using the same technique. No comparison either has been done between the existing data, and no dimensionless formulation exists that has been tested on several cases. Finally, as local characteristics of two-phase flow are now available using optical probes, the relation between these characteristics and the resulting forces can be explored.

In Section 2, new experiments on a bend and a tee are described. The dimensionless formulation of Yih and Griffith [2] is extended in Section 3 to include all experiments mentioned above. Finally, in Section 4 a local measurement of the time-dependent void fraction is used to reconstruct the measured excitation.

2. Experiments

2.1. Experimental set-up

An air–water loop was constructed to simulate two-phase flow. Air from the local compressed air service is mixed with water to produce two-phase flow. A mixer made of a fine screen is used at the inlet of the test section to homogenize the mixture. After the test section, the flow is discharged in a tank where the air escapes. In the performed tests, the volumetric flow rates of air and water were varied from 0.1 to 10.4, and from 0.17 to 1.25 L/s, respectively. Two parameters are used to specify the flow conditions [12]: the volumetric quality (or homogeneous void fraction), β , and the superficial or homogeneous velocity, referred simply as velocity in this

paper, j , defined respectively as

$$\beta = \frac{Q_g}{Q_g + Q_l}, \quad j = \frac{Q_g + Q_l}{A}, \quad (1)$$

where A is the total flow area, Q_g and Q_l stand for the volumetric flow rate of air and water, respectively. A set of 11 two-phase mixtures was tested with two different volumetric qualities $\beta = 50\%$ and $\beta = 75\%$ and velocity j varying from 2 to 6 m/s in the first case and from 2 to 12 m/s in the second case. These conditions are selected so that the main flow patterns, according to the map of Taitel et al. [13], would be bubbly or churn flow. A larger set of experiments is reported in Ref. [3], with tests in other flow regimes.

Flow is carried by a transparent PVC tube of internal diameter $D = 20.6$ mm, mounted vertically. Two set-ups are considered. First, a U-tube configuration, Fig. 1a, is made of two sharp bends (radius of curvature $R = D/2$) at distance of $L = 300$ mm. Second, a Tee configuration, Fig. 1b, is made with two equal short branches of the same diameter as the vertical pipe. In both configurations a piezoelectric force sensor was used to measure the force exerted by the flow on the tube. In the U-Tube configuration the force sensor is attached horizontally on one side to the first bend and on the other side to a rigid bracket, Fig. 1a. In the Tee configuration the force sensor is attached vertically on the central part of the tee junction, Fig. 1b. Here, a small sliding device decouples the measured force from the tension in the vertical pipe.

For the sake of comparison between these two configurations and with the previous results in Refs. [2,4], we define an equivalent bend force F_B , Fig. 1c, as the fluctuating part of the flow-induced force projected on the

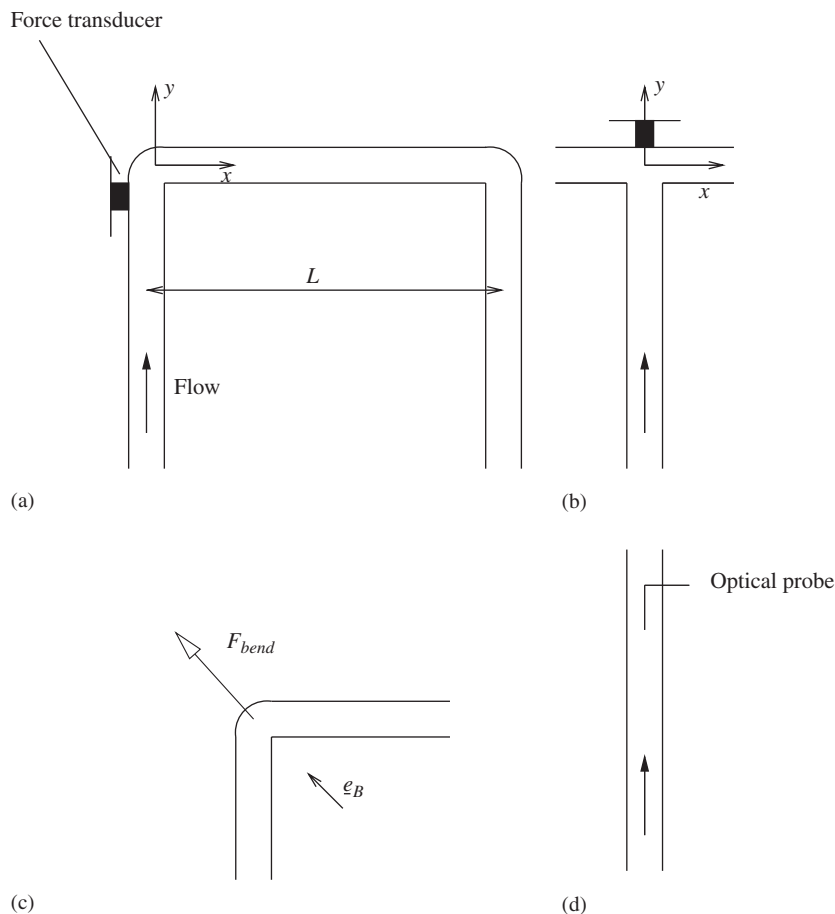


Fig. 1. Experimental apparatus. (a) U-bend configuration; (b) tee configuration; (c) definition of the equivalent bend force; and (d) optical probe position.

outward oriented median of a bend, \underline{e}_B . For the U-bend configuration, the measured force F_X results from the sum of forces exerted at the two bends, each being projected on the horizontal axis x ,

$$F_X(t) = -\frac{1}{\sqrt{2}}F_{B,1}(t) + \frac{1}{\sqrt{2}}F_{B,2}(t), \tag{2}$$

where the subscripts 1,2 refer to each bend. The power spectral density (PSD) and the rms value of the measured force are related to those of the bend force. If it is assumed that $F_{B,1}$ and $F_{B,2}$ are of equal magnitude and fully decorrelated then the PSD and the rms force read

$$\Phi_X(f) = \Phi_B(f), \quad F_X^{\text{rms}} = F_B^{\text{rms}}. \tag{3}$$

If some correlation exists between the forces at the two bends, as a result of convection of the flow structure between them, the measured force will underestimate the equivalent bend forces, as correlated force would cancel each others. Following Ref. [2], this effect can be estimated and has not been found to be of importance here. In the Tee configuration the measured force in the y direction is equivalent to the projection of a bend force so that

$$F_Y(t) = \frac{1}{\sqrt{2}}F_B(t), \quad \Phi_Y(f) = \frac{1}{2}\Phi_B(f), \quad F_Y^{\text{rms}} = \frac{1}{\sqrt{2}}F_B^{\text{rms}}. \tag{4}$$

In addition to the measurement of forces an optical probe was used to measure the local properties of two-phase flow. The probe, made of an optical fibre of 0.17 mm diameter with a conical tip, acted as a phase sensor based on the different level of light reflection between air and water. Its principle of operation is the same as described in Ref. [14]. The probe was inserted in a vertical straight tube made of the same material and of same diameter as the U-tubes, Fig. 1d. Probe data were recorded for a period of 200 s for each run. As a result the

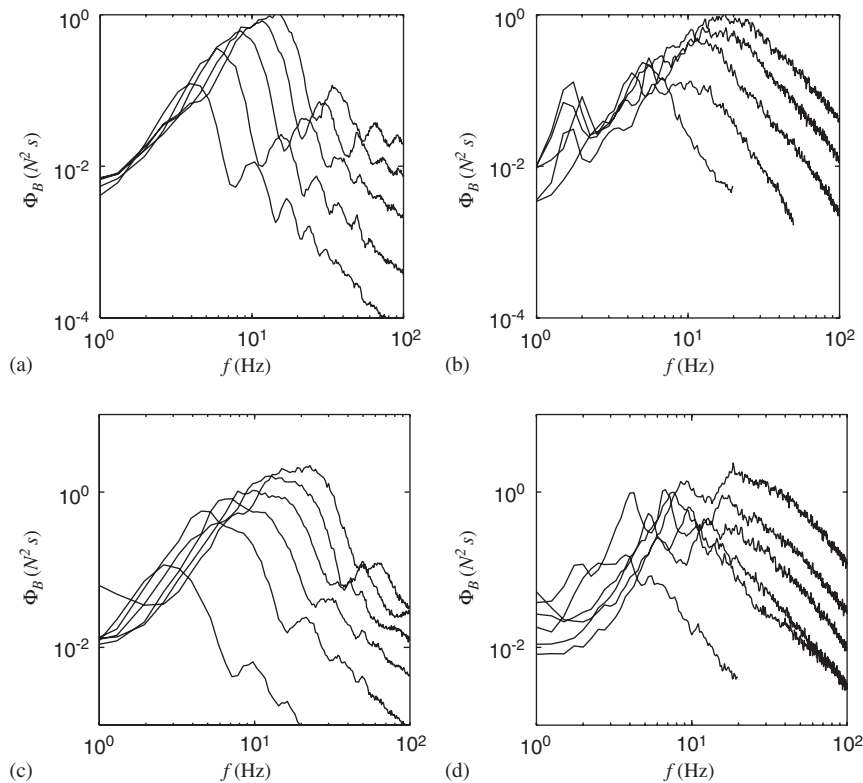


Fig. 2. Spectrum of equivalent bend forces. (a) U-bend, $\beta = 50\%$; (b) Tee, $\beta = 50\%$; (c) U-bend, $\beta = 75\%$; (d) Tee, $\beta = 75\%$. In each graph the spectra are given for the following velocities: $j = 2, 3, 4, 5, 6$ m/s for $\beta = 50\%$, and $j = 2, 4, 6, 8, 10, 12$ m/s for $\beta = 75\%$. Increasing spectral levels correspond to increasing velocities.

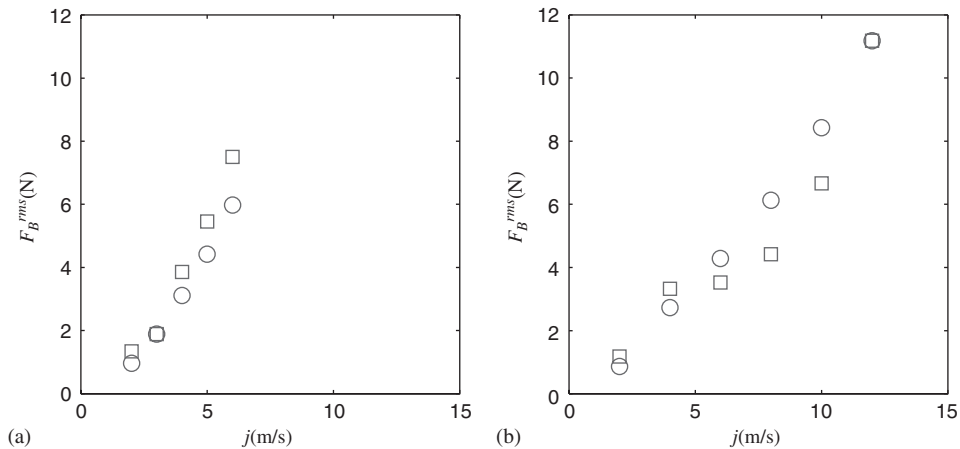


Fig. 3. rms value of the equivalent force as a function of the flow velocity. (a) $\beta = 50\%$; (b) $\beta = 75\%$; \circ , U-bend; \square , Tee.

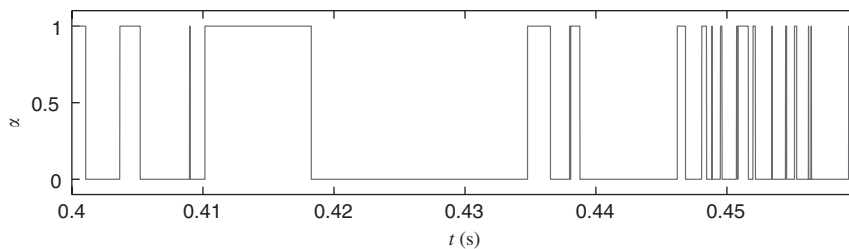


Fig. 4. Typical evolution with time of the instantaneous void fraction α measured by the optical probe, $\beta = 50\%$, $j = 6$ m/s.

instantaneous local void fraction $\alpha(t)$ is derived, being equal either to zero or one, corresponding to the presence of liquid or gas. Four flow conditions were tested, corresponding to the minimum and maximum values of β and j .

2.2. Experimental results

In the two configurations, Tee and U-bend, the equivalent bend force as a function of time is derived from the measured forces. The corresponding PSD are shown in Fig. 2. The rms value of the equivalent bend force with the flow velocity j is plotted in Fig. 3. In these results it appears that: (a) the forces caused by the two-phase flows at $\beta = 50\%$ and $\beta = 75\%$ are similar, though different in magnitude, (b) for a given void fraction and flow velocity forces on bends and on a tee are similar if referred to an equivalent bend force, (c) the effect of the flow velocity is continuous in this range of parameters, (d) the PSD shows a pronounced dominant frequency that varies with the flow velocity.

A typical evolution with time of the local void fraction $\alpha(t)$ measured by the optical probe is shown in Fig. 4.

3. Dimensionless forces

3.1. RMS of forces

In the presentation of their experimental force measurement on a Tee for different tube diameters, void fractions and flow velocities, Yih and Griffith [2] proposed to use the following dimensionless form:

$$\frac{F^{rms}}{F^{stat}} We^{0.4} = A(\beta), \tag{5}$$

where $F^{\text{stat}} = \rho_L(1 - \beta)j^2(\pi D^2/4)$ is the stationary component of the force, the Weber number is defined by

$$We = \frac{\rho_L j^2 D}{\sigma}; \tag{6}$$

and $A(\beta)$ is a function of void fraction given graphically in Ref. [2]. The Weber number scales the dynamic pressure with the effect of surface tension. This relation was found to give a reasonable collapse of all data points in a range of void fraction from 55% to 98%. We only use here data for void fractions below 75% to be consistent with our experiments. Moreover, only in that range can the original data be reconstructed from the dimensionless results. These experiments were made with a diameter of 6.35 mm and a velocity of 16.5 m/s.

More generally, if it is assumed that the viscosity of the liquid μ , gravity g and the densities of both phases ρ_L, ρ_g , all influence the magnitude of the forces, the corresponding dimensional relation should read

$$F_{\text{rms}} = b(j, \beta, D, \rho_L, \rho_g, \sigma, \mu, g), \tag{7}$$

where b is the unknown function of all these dimensional parameters. Using standard dimensional analysis, as in de Langre and Villard [15] for the case of external flow, this may equivalently be written as

$$\frac{F_{\text{rms}}}{\rho_L(1 - \beta)j^2(\pi D^2/4)} = B\left(\beta, \frac{\rho_L}{\rho_g}, We, Re, Fr\right), \tag{8}$$

where the Reynolds and Froude numbers are, respectively,

$$Re = \frac{\rho_L j D}{\mu}, \quad Fr = \frac{j}{\sqrt{\rho_L g}}; \tag{9}$$

and where B now only depends on the dimensionless parameters. Clearly, Eq. (8) is a generalization of Eq. (5). Using the experimental results presented in the preceding section as well as from the conclusions of Yih and Griffith [2] and of Tay and Thorpe [4] the effect of each parameter may be assessed as follows:

- (a) The flow velocity j was found to influence the force as $j^{1.2}$ in Ref. [2] and as $(j_0 + j)^2$ in Ref. [4], j_0 being a constant. The variation as $j^{1.2}$ is compatible with our tests, Fig. 3, though a slightly higher exponent might be more appropriate (see Ref. [3] for a detailed analysis). This dependence would imply that the function B in Eq. (8) varies either as $We^{-0.4}$ or $Re^{-0.8}$ or $Fr^{-0.8}$ or any combination of these such that the resulting variation in j is, in this combination, $j^{-0.8}$.
- (b) When the diameter was varied by a factor of 4 in Ref. [2], for higher void fractions, the force was found to vary as $D^{1.6}$. This is not compatible with the dependences in Reynolds and Froude number mentioned above, which would yield a variation of $D^{1.2}$ and $D^{2.4}$, respectively.
- (c) When surface tension was varied by 35% in the experiments of Tay and Thorpe [4] a very small variation in the level of forces was found. This is compatible with a variation as $We^{-0.4}$ where the surface tension, acts as $\sigma^{0.4}$ only.
- (d) Similarly when viscosity was varied by a factor of 2.6 in Ref. [4] a small variation in the level of forces was found. This is compatible with no significant dependence with the Reynolds number.
- (e) In terms of the effect of gravity, it should be noted that the experiments by Tay and Thorpe [4] are made with a horizontal pipe, whereas those of Yih and Griffith [2], as well as those of the present work, are made with a vertical pipe. Gravity is known to play an important role on the flow structure in both configuration, but differently. As we wish to compare vertical and horizontal test we assume as a first approximation that there is no dependence of the force with the Froude number.
- (f) The effect of the mass ratio ρ_L/ρ_g was analysed by Yih and Griffith [2], for higher void fractions. By doubling the pressure and thus doubling the gas density the magnitude of forces was reduced by about 15%. The dependence with ρ_L/ρ_g in that range is therefore small and may be discarded. When considering higher gas density, such as in vapour, using the density of air probably yields an overestimation of the forces. This has been observed before in modelling the effect of two-phase flow across tube bundles, see Refs. [1,9].

(g) Finally, in terms of the effect of void fraction the results of Fig. 3 show that from 50% to 75% the magnitude of the force varies slightly. In Ref. [2] less than a factor of 2 is found in the function A of Eq. (5). We may assume that B varies like $1/(1 - \beta)$.

From these considerations, it appears that the formulation proposed by Yih and Griffith may be extended as

$$\frac{F_{rms}}{\rho_L(1 - \beta)j^2(\pi D^2/4)} = \frac{B}{1 - \beta} We^{-0.4} \tag{10}$$

which also reads simply

$$\overline{F_{rms}} = \frac{F_{rms}}{\rho_L j^2(\pi D^2/4)} = C We^{-0.4}, \tag{11}$$

where C is a constant.

In Fig. 5 we show the dependence of this dimensionless rms $\overline{F_{rms}}$ force with the Weber number. On the same graph are plotted experiments in this range of void fraction: those of Yih and Griffith [2], those of Section 2 and those of Tay and Thorpe [4]. For these latter experiments a conversion is needed to derive the rms value of the force from its maximum value, reported in Ref. [4]. In our experiments we found $F^{max}/F^{rms} \simeq 5$, which is used here. Note that this ratio may depend on the flow regime.

Eq. (11) is found to be a reasonable approximation for all these results, with $C = 10$. It is remarkable that this relation allows to compare tests with significant differences in terms of diameter (from 6 to 70 mm), flow velocity (1 to 17 m/s), surface tension (0.05–0.07 N/m), viscosity (10^{-6} – 2.6×10^{-6} Kg/ms) and geometry (tee, bend, U-bend). Results from tests at a void fraction of 25%, not shown the figure, also follow the same trend, see Ref. [3].

The experimental data on pressure fluctuation given by Wang and Shoji [6] may also be analysed using this approach. We consider their case of symmetric flow, $w_3/w_1 = 0.5$, with water and gas superficial velocities of 0.14 and 0.94 m/s, respectively, as described in Fig. 6b of Ref. [6]. We may estimate the fluctuating force by

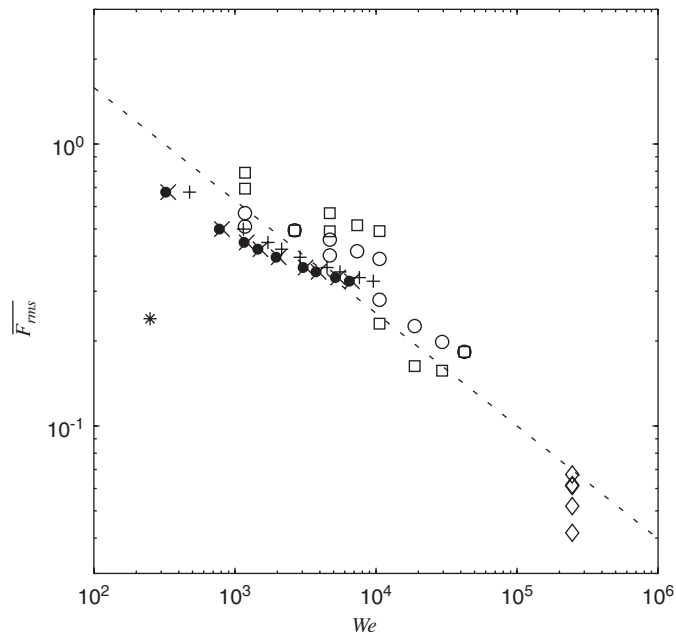


Fig. 5. Dimensionless rms force on a bend as a function of the Weber number. Present test: \circ , U-bend; \square , Tee. Tests by Yih and Griffith [2]: \diamond . Tests by Tay and Thorpe with water, water with isopropanol surfactant and water with glycerol solution, respectively [4]: \bullet , \times , $+$. Force estimated from pressure data in a test by Wang and Shoji [6]: $*$. Extension of the formulation of Yih and Griffith [2], Eq. (11) with $C = 10$, (- -).

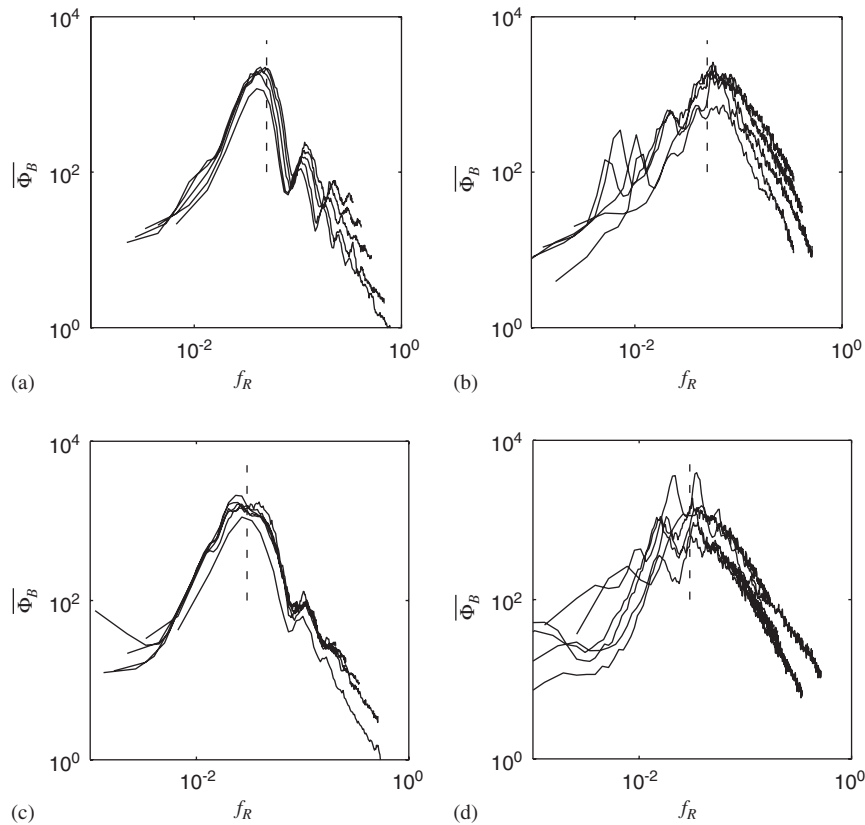


Fig. 6. Dimensionless spectrum of equivalent bend forces as a function of the reduced frequency. (a) U-bend, $\beta = 50\%$, (b) Tee, $\beta = 50\%$, (c) U-bend, $\beta = 75\%$, (d) Tee, $\beta = 75\%$. (—) dominant frequency.

integrating the measured fluctuating pressure over an area equal to that of the pipe section. This results in a dimensionless fluctuating force $\overline{F}_{rms} = 0.24$ with a Weber number of $We = 250$. In Fig. 5 the corresponding data point is lower than our proposed relation. Note that the void fraction $\beta = 0.87$ is higher than those we considered in our experiments. Moreover Eq. (11) remains an upper bound.

3.2. Dimensionless spectrum

In terms of the spectral characteristics of the forces, few data are available. The spectra computed in Ref. [2] are not accurately defined, due to the rather simple data processing available in the late 60s. Only the results of our test are reported here. Using the dimensional analysis presented above, the dimensionless form of the PSD must be such that its integration over frequency yields the dimensionless rms value. This requires that

$$\frac{\Phi_B}{(\rho_L j^2 D^2)^2} f_0 We^{0.8} = E\left(\frac{f}{f_0}\right), \tag{12}$$

where f_0 is a reference frequency and $E()$ is a function of the dimensionless frequency f/f_0 . A natural reference frequency is $f_0 = j/D$. In Fig. 6 the PSD of the equivalent forces, given in Fig. 2, are shown now in dimensionless form using

$$\overline{\Phi_B} = \frac{\Phi_B}{(\rho_L j^2 D^2)^2} \left(\frac{j}{D}\right) We^{0.8}, \quad f_R = \frac{fD}{j}, \tag{13}$$

where f_R is commonly defined as the reduced velocity. It is found that for a given void fraction the dependence with velocity is satisfactorily taken into account.

On these dimensionless spectra a dominant frequency is well defined at $fD/j \simeq 0.05$ for $\beta = 50\%$ and $fD/j \simeq 0.03$ for $\beta = 75\%$. The Strouhal number defined by Azzopardi and Baker [16] for the dominant frequency of fluctuations in a two-phase flow is

$$S_T = \frac{fD}{j(1 - \beta)}. \tag{14}$$

Its value is here approximatively $S_T = 0.10$ for $\beta = 50\%$ and $S_T = 0.12$ for $\beta = 74\%$. This falls in the range of Strouhal numbers for this range of void fractions, as given in Ref. [16], showing that periodicity of the force exerted by the two-phase flow is the result of a periodicity in the flow structure. Here again some data from Wang and Shoji [6] may be considered. In the nearly symmetric case of Fig. 8b in Ref. [6], the dominant frequency is about 2 Hz, so that the Strouhal number is $S_T = 0.33$. This is compatible with the data given in Ref. [16] for this range of void fraction (here $\beta = 0.91$).

4. Relation with local void fraction

Following Yih and Griffith [2] the fluctuating force may be related to the variation with time of the fluid momentum. The equivalent bend force is given by the momentum balance equation, projected on the axis \underline{e}_B defining F_B , Fig. 1c. It reads

$$F_B(t) = \frac{1}{\sqrt{2}} \int_{\text{Inlet}} \rho j^2 dA + \frac{1}{\sqrt{2}} \int_{\text{Outlet}} \rho j^2 dA - \frac{\partial}{\partial t} \left[\int_{\text{Bend volume}} \rho \underline{j} \cdot \underline{e}_B dV \right], \tag{15}$$

where the first two surface integrals relate to the flow characteristics at the entrance and exit of the bend, the third one being a volume integral over the whole fluid domain in the bend. This is identical to the formulation used by Yih and Griffith [2] to relate the force exerted by the flow on a tee to variations in void fractions, except for gravity effects which are neglected here. It is also equivalent to the formulation developed by Tay and Thorpe [4,5], named piston flow model (PFM), except for the pressure gradients due to friction which are neglected here.

Though the flow regimes in our experiments are bubbly and churn flows we model it here as alternative slugs of liquid and gas, as measured by the optical probe. From this simplifying assumption the density is homogeneous across a section of the pipe and is equal to

$$\rho(t) = \rho_L(1 - \alpha(t)), \tag{16}$$

where the gas density has been neglected. Considering that the void fraction pattern is convected by the flow velocity j , the density at the inlet, outlet and inside the bend are related by time lags only. Using Eqs. (15) and

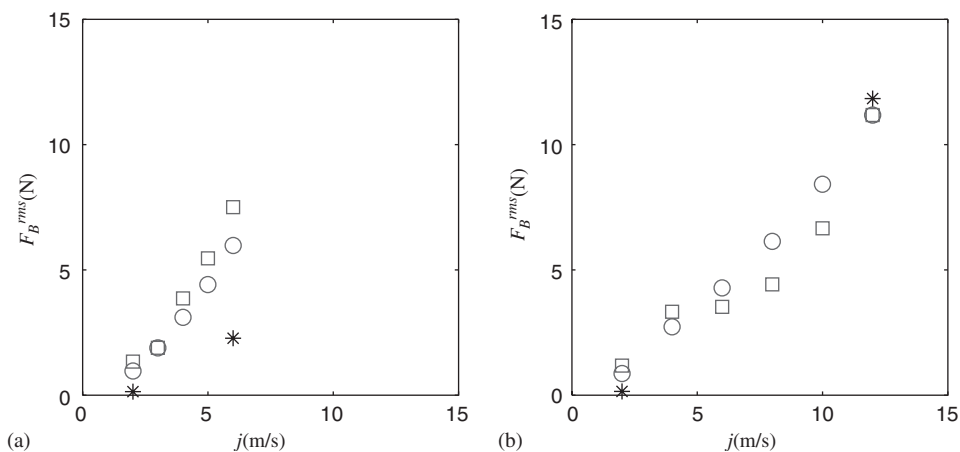


Fig. 7. rms value of the equivalent force as a function of the flow velocity. (a) $\beta = 50\%$; (b) $\beta = 75\%$; \circ , U-bend; \square , Tee; *, force estimated using the local measured void fraction.

(16) we have

$$\frac{F_B(t)}{\rho_L j^2 \pi D^2 / 4} = \frac{2 - \alpha(t) - \alpha(t - \delta)}{\sqrt{2}} + \int_0^\delta \left(\frac{\partial \alpha}{\partial t} \right)_{t-\tau} \cos\left(\frac{\pi}{4} + \frac{\tau j}{R}\right) d\tau, \quad (17)$$

where the time lag between the inlet and outlet is $\delta = \pi R / (2j)$. The corresponding rms values are plotted Fig. 7, in comparison with the direct measurement of the force. The order of magnitude is similar, at least for the higher velocities.

5. Concluding remarks

When considering bends and tees in various geometrical and flow configurations a relation is found between the fluctuating forces caused by the two-phase flow and the characteristics of the flow. This relation is here expressed in a dimensionless form for application to other conditions. The magnitude of the forces may also be related to local fluctuations of void density in the mixture.

In some particular cases, such as in the experiments of Tay and Thorpe [4] with slugs entering a horizontal bend, a much closer agreement was found between the measured forces and those derived from the measured characteristics of the slugs using a momentum equation. In such cases the flow structure is indeed well defined and the precise geometry of the boundary between the liquid and gas phases of a given slug can be tracked, as shown in Ref. [4]. When vertical flows are considered, with bubbly and churn regimes, the dynamics of the phases is much more complex. The corresponding momentum balance would require much more information on this dynamics to have the same accuracy. In practical applications in the design of piping systems, bends and tees follow horizontal and vertical sections, depending on their location. It is then recommended to use Eq. (11) as a first approximation of the magnitude of forces that can be expected. The corresponding spectral content is given by Fig. 6. For higher void fractions some preliminary comparisons following the methodology used here show a more pronounced dependence of the forces on the geometry, orientation and flow conditions, which is probably an effect of flow regime.

Acknowledgements

The authors are grateful to Benedict Besner, Thierry Lafrance and Sylvain Luc for their support in the experimental work, and to Dr. Njuki W. Mureithi for his valuable comments. Emmanuel de Langre gratefully acknowledges the support of the French DGA Grant 03 60 00 063 and of Ecole polytechnique Montréal for his sabbatical stay in the BWC/AECL/NSERC Chair of Fluid-Structure Interaction.

References

- [1] M.J. Pettigrew, C.E. Taylor, Two-phase flow-induced vibration: an overview, *Journal of Pressure Vessel Technology* 116 (1994) 233–253.
- [2] T.S. Yih, P. Griffith, Unsteady momentum fluxes in two-phase flow and the vibration of nuclear system components, *Proceedings of the International Conference on Flow-Induced Vibrations in Reactor System Components*, Argonne IL, 1970, Report ANL-7685, pp. 91–111.
- [3] J.L. Riverin, M.J. Pettigrew, Fluctuating forces in U-tubes subjected to internal two-phase flow, *Proceedings of PVP2005 2005 ASME Pressure Vessels and Piping Division Conference*, Denver, Colorado, USA, July 17–21, 2005, paper PVP2005-71424.
- [4] B.L. Tay, R.B. Thorpe, Effect of liquid physical properties on the forces acting on a pipe bend in gas–liquid slug flow, *Chemical Engineering Research and Design* 82 (2004) 344–356.
- [5] B.L. Tay, R.B. Thorpe, Forces on a pipe bend due to slug flow, *Proceedings of the Third North American Multiphase Technology Conference*, Banff, 2002, pp. 281–300.
- [6] S.F. Wang, M. Shoji, Fluctuation characteristics of two-phase flow splitting at a vertical impacting T-junction, *International Journal of Multiphase Flow* 28 (2002) 2007–2016.
- [7] S.F. Wang, M. Ozawa, M. Shoji, Fluctuation gas–liquid two-phase flow splitting at a vertical T-junction, *Proceedings of UK/Japan Two-Phase Flow Meeting*, Guildford, UK, 14–15 April 2003.
- [8] S.F. Wang, R. Mosdorf, M. Shoji, Nonlinear analysis on fluctuation feature of two-phase flow through a T-junction, *International Journal of Heat and Mass Transfer* 46 (2003) 1519–1528.

- [9] D. Gueyffier, J. Li, A. Nadim, R. Scardovelli, S. Zaleski, Volume-of-fluid interface tracking with smoothed surface stress methods for three-dimensional flows, *Journal of Computational Physics* 152 (1999) 423–456.
- [10] S. Supa-Amornkul, F.R. Steward, D.H. Lister, Modeling two-phase flow in pipe bends, *Journal of Pressure Vessel Technology* 127 (2005) 204–209.
- [11] D. Adechy, R.I. Issa, Modelling of annular flow through pipes and T-junctions, *Computers and Fluids* 33 (2004) 289–313.
- [12] J.G. Collier, J.R. Thome, *Convective Boiling and Condensation*, third ed., Oxford University Press, Oxford, 1994.
- [13] Y. Taitel, D. Barnea, A.E. Dukler, Modeling flow pattern transitions for steady upward gas–liquid flow in vertical tubes, *AIChE Journal* 26 (1980) 345–354.
- [14] D. Morris, A. Teyssedou, J. Lapierre, A. Tapucu, Optical fiber probe to measure local void fraction profiles, *Applied Optics* 26 (1987) 4660–4664.
- [15] E. de Langre, B. Villard, An upperbound on random buffeting forces caused by two-phase flows across tubes, *Journal of Fluids and Structures* 12 (1998) 1005–1023.
- [16] B.J. Azzopardi, G. Baker. Characteristics of periodic structures in gas/liquid two-phase flow, *Proceedings of UK/Japan Two-Phase Flow Meeting*, Guildford, UK, 14–15 April 2003.